

# Nickel Oxide Nanoparticles Modified Gold Electrode for Fractional Determination of Dopamine and Ascorbic Acid<sup>1</sup>

Mohamed I. Awad<sup>a, b, \*, \*\*</sup>, B. A. AL Jahdaly<sup>a</sup>, Mohammed A. Kassem<sup>a, c</sup>, and Omar A. Hazazi<sup>a</sup>

<sup>a</sup>Chemistry Department, Faculty of Applied Sciences, Umm Al-Qura University, Makkah Al-Mukarramah, Saudi Arabia Kingdom

<sup>b</sup>Chemistry Department, Faculty of Science, Cairo University, Cairo, Egypt

<sup>c</sup>Chemistry Department, Faculty of Science, Benha University, Benha, 13518 Egypt

\*e-mail: mawad70@yahoo.com

\*\*e-mail: miawad@uqu.edu.s

Received September 22, 2016; in final form, May 5, 2018

**Abstract**—Dopamine and ascorbic acid has been fractionally determined at nickel oxide nanoparticles (**nano-NiO<sub>x</sub>**) modified polycrystalline gold electrode (**poly-Au**), nano-NiO<sub>x</sub>/Au, with high selectivity using voltammetric techniques. Nano-NiO<sub>x</sub>/Au electrode, fabricated electrochemically, could resolve the overlapping obtained at the bare poly-Au electrode. Nano-NiO<sub>x</sub>/Au electrode was prepared by cycling of potential of Au electrode in diluted Watts bath in the potential range between 0.0 and –1.0 V vs. Ag/AgCl (KCl sat.), and was characterized morphologically and electrochemically. Effect of loading level of nickel was examined by changing the number of potential cycles for the deposition of nickel nanoparticles, i.e., 1, 2 and 5 potential cycles were used. Also the effects of the electrooxidation of the thus deposited nickel nanoparticles and pH of the electrolyte on the voltammetric behavior were investigated. The good calibration curve of an acceptable rectilinear range is obtained at nano-NiO<sub>x</sub>/Au electrode in which nano-Ni was prepared by two potential cycles and subsequently electro-oxidized in KOH solution.

**Keywords:** nanoparticles, nickel oxide, electrocatalysis, electroanalysis, dopamine

**DOI:** 10.1134/S1061934818120067

Applications of nanostructured surfaces in diverse fields are exponentially increasing. One of the most important applications is biomolecules sensing via tuning of the interfacial properties of modified electrodes, and consequently the electrocatalytic activity. The determination of species such as dopamine (**DA**), naturally occurring catecholamine, are particularly important for neuroscientists. Dopamine is a key neurotransmitter that is vital for the function of the central nervous system and control of hormonal and cardiovascular systems. Anomalous levels of DA can lead to disorders such as schizophrenia, senile dementia and Parkinson's disease [1–3].

On the other hand, metal and metal oxide nanoparticles have received considerable attention in recent years, as they have high catalytic properties compared with their bulk counterparts. They have size dependent unique chemical, electrical and optical properties and are very promising for practical applications in diverse fields, like electronic nanodevices, molecular catalysts, multifunctional reagents and biosensors [4–9].

In the present work we examine the possible fractional determination of DA and ascorbic acid (**AA**), coexisting in the extracellular fluids, at nickel oxide nanoparticles modified gold electrode (nano-NiO<sub>x</sub>/Au) with different loading. Results are compared to those obtained at the poly-Au electrode on which the electrochemical responses of the two species overlap. In addition, bare gold electrodes suffer from the fouling effect due to accumulation of the oxidized product [10]. Also, AA oxidation is homogeneously catalyzed by the oxidized DA [11]. Both species were simultaneously determined by using several techniques [12–16] including voltammetric methods with their known selectivity and simplicity [17–19]. Ohsaka et al. [20, 21] utilized the different interactions of the two species with the thiol modified electrodes for the selective determination of the two species. However, thiol modified gold electrodes are not so stable, as the assembled thiol molecules might desorb with several potential scans, or when potential of the electrode is excursed at higher anodic potential. The present modification is comparatively more stable and might give the possibility of using nano-NiO<sub>x</sub>/Au electrode for the detection of DA and AA in their

<sup>1</sup> The article is published in the original.

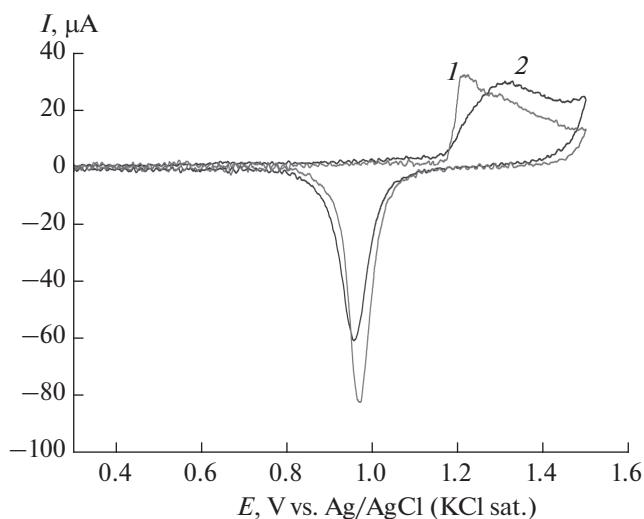


**Fig. 1.** Cyclic voltammograms obtained at bare polycrystalline gold (1) and nano-Ni/Au (2) electrodes in  $\text{N}_2$ -saturated 0.5 M  $\text{H}_2\text{SO}_4$  solution. Scan rate 100 mV/s.

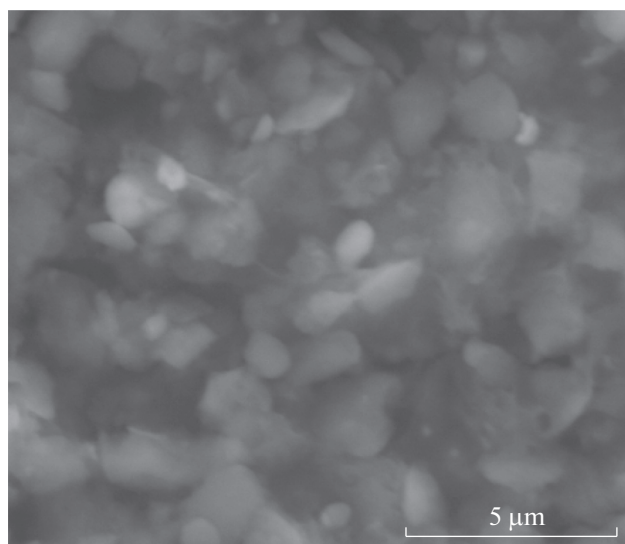


**Fig. 2.** SEM image obtained for nano-Ni/Au electrode prepared by two potential cycles, as explained in the experimental section.

coexistence at considerable selectivity and sensitivity. It relies on the interaction of ascorbic acid with  $\text{NiO}_x/\text{Au}$  electrode.

## EXPERIMENTAL

**Reagents and solutions.** All experiments were performed using analytical grade chemicals without further purification; their solutions were prepared using bidistilled water. Dopamine and ascorbic acid standard solutions were prepared in bidistilled water.

**Electrodes.** The polycrystalline gold (poly-Au) electrode (1.6 mm in diameter) was polished to mirror-like with alumina powder (down to 0.06  $\mu\text{m}$ ) and then rinsed ultrasonically for 10 min in bidistilled water for removing any physically adsorbed species. Next, it was electrochemically pretreated in  $\text{N}_2$ -saturated 0.05 M  $\text{H}_2\text{SO}_4$  solution by repeating the potential scan in the potential ranges of  $-0.2$  to  $1.5$  V vs. Ag/AgCl (KCl sat.) until the cyclic voltammetric (CV) characteristic of a clean Au electrode was obtained.

**Preparation of nano- $\text{NiO}_x/\text{Au}$  electrode.** Nickel was electrodeposited from Watts bath [22]; ( $\text{NiSO}_4 \cdot 6\text{H}_2\text{O}$  240 g/L +  $\text{NiCl}_2 \cdot 6\text{H}_2\text{O}$  45 g/L +  $\text{H}_3\text{BO}_3$  30 g/L), after being diluted 2000-fold with  $\text{H}_2\text{SO}_4$  solution, by cycling the potential in the range 0 to  $-1.0$  V. Then the electrode was subjected to several potential cycles in 0.1 M KOH for oxidizing the thus deposited nickel.

**Measurements.** Electrochemical measurements were performed using a PGSTAT30 potentiostat/galvanostat (Netherlands) controlled by General Purpose Electrochemical Systems (GPES) and Frequency Response Analyzer (FRA) software. The working electrode and the counter electrode (a platinum spiral wire) were separated by a porous glass. An

Ag/AgCl (KCl sat.) electrode was used as the reference electrode. A conventional three-electrode cell of around 20 mL was used for the cyclic voltammetric measurements. All electrochemical measurements were conducted under nitrogen saturated solutions.

**Scanning electron microscopy (SEM) measurements** were carried out using a Hitachi microscope. An accelerating voltage of 20 kV was used for all the images done in this work.

## RESULTS AND DISCUSSION

**Cyclic voltammetry.** Figure 1 shows cyclic voltammograms obtained at bare poly-Au (curve 1) and nickel nanoparticles modified gold electrode, nano-Ni/Au (curve 2) in  $\text{N}_2$ -saturated 0.05 M  $\text{H}_2\text{SO}_4$ . The characteristic CV of a clean poly-Au electrode clearly shows in curve 1 the oxidation peak (at ca. 1.1–1.5 V vs. Ag/AgCl) that corresponds to the formation of gold oxide monolayer, coupled with a reduction peak centered at ca. 0.9 V [23]. It has been reported that the oxidation peak corresponds to the oxidation of the different facets of the poly Au electrode, i.e., Au (111), Au (110) and Au (100) facets [23]. The decrease in both peaks, i.e., oxidation and reduction, shown in the case of nano- $\text{NiO}_x/\text{Au}$  electrode (curve 2) reflects the deposition of nickel onto poly-Au electrode. The deposition of nickel onto poly-Au electrode is revealed from the SEM image (Fig. 2, in which nickel is deposited via two potential cycles onto the underlying poly-Au electrode, as explained in the experimental section.

Figure 3 shows cyclic voltammograms obtained at bare polycrystalline gold (2), nano-Ni/Au (3) and nano- $\text{NiO}_x/\text{Au}$  (4) electrodes in  $\text{N}_2$ -saturated phosphate buffer solution (pH 7.25) containing 0.25 mM

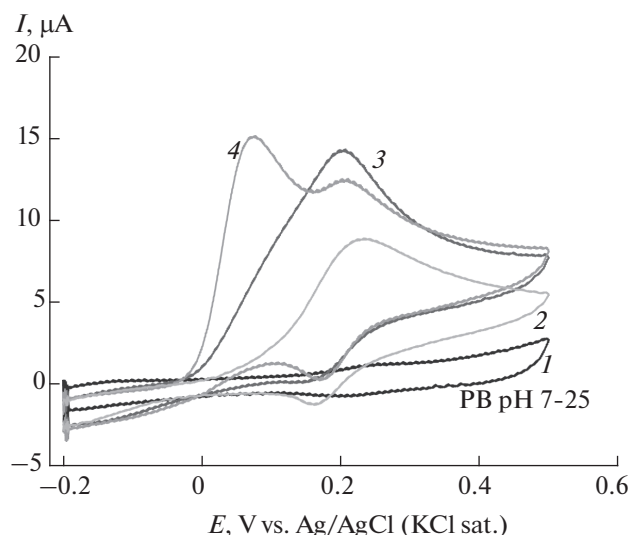


**Fig. 3.** Cyclic voltammograms obtained at bare polycrystalline gold (2), nano-Ni/Au (3) and nano-NiO<sub>x</sub>/Au (4) electrodes in N<sub>2</sub>-saturated phosphate buffer solution (pH 7.25) (1) containing 0.25 mM DA + 1.0 mM AA (2–4). Nano-Ni/Au was prepared using two potential cycles. Scan rate 100 mV/s.

DA + 1.0 mM AA. Curve 1 is the blank response obtained at bare Au electrode. Inspection of this figure reveals that (i) at bare Au electrode (curve 2) the electrochemical responses of DA and AA are overlapped, and only one anodic peak is obtained over a wide potential range (0–0.5 V). This anodic peak is coupled by one cathodic peak centered at 0.16 V and probably corresponds to the dopamine reduction. In curve 3 which is obtained at nano-Ni/Au electrode, the two peaks for DA and AA start to be separated. In addition, the onset potential of AA is shifted negatively.

The two ill-defined peaks corresponding to DA and AA are obtained at 0.08 and 0.20 V, respectively. It is noteworthy to mention that the anodic peak potential (ca. 0.2 V) corresponding to the oxidation of dopamine is almost constant at the studied electrodes, i.e. at the bare, nano-Ni/Au and nano-NiO<sub>x</sub>/Au electrodes. Modification of electrode significantly affects the oxidation of ascorbic acid, but not the oxidation of DA. At nano-NiO<sub>x</sub>/Au (Fig. 3, curve 4) the peak of AA is shifted negatively and separated to a large extent from the DA oxidation peak. It has been reported that nickel oxide rather than metallic nickel is the appropriate electrocatalyst for the oxidation of hydroxyl compounds [24]. Thus, the negative shift of AA oxidation at nano-NiO<sub>x</sub>/Au electrode could be attributed to the enhanced adsorption of AA.

To examine the effect of loading of nickel oxide, nano-Ni was deposited using different potential cycles and subsequently oxidized by potential cycling of the thus prepared electrodes in KOH solution, and results are shown in Fig. 4, in which the cyclic voltammo-

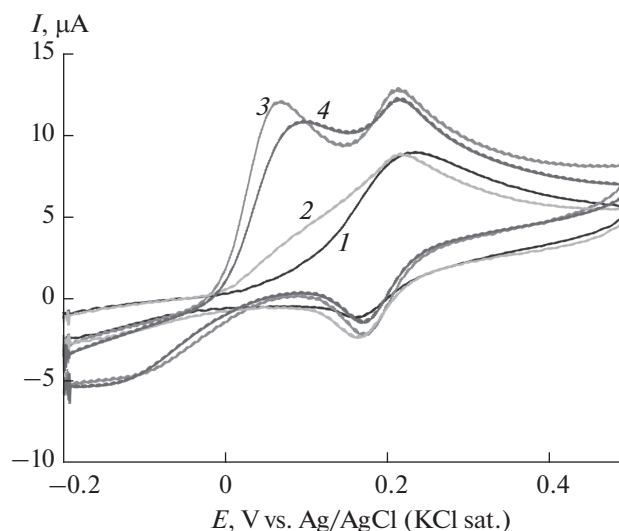


**Fig. 4.** Cyclic voltammograms obtained at bare Au (1) and nano-NiO<sub>x</sub>/Au (2–4) electrodes in N<sub>2</sub>-saturated phosphate buffer solution (pH 7.25) containing 0.25 mM DA + 1.0 mM AA. Nano-NiO<sub>x</sub>/Au electrodes were prepared by one (2), two (3) and five (4) potential cycles. Scan rate 100 mV/s.

grams obtained at bare Au (1) and nano-NiO<sub>x</sub>/Au (2–4) electrodes in phosphate buffer solution containing 0.25 mM DA + 1.0 mM AA are given. Nano-NiO<sub>x</sub>/Au were prepared as mentioned in the experimental section by one potential cycle (2), 2 cycles (3) and 5 cycles (4). As clearly shown, the loading level of NiO<sub>x</sub> is inherently controlling; while nano-NiO<sub>x</sub>/Au electrode prepared by 2 potential cycles nicely separate the two oxidation peaks of DA and AA, the electrode prepared by one potential cycle is insufficient to completely separate the two oxidation peaks, and the one prepared by 5 potential cycles, even though it could separate the two peaks, but the separation is not as much as the one obtained in the case of the modified electrode prepared by 2 potential cycles. Hence, the loading prepared by two potential cycles will be used hereafter as the optimum one.

It is noteworthy to mention that the combination of nickel nanoparticles and the gold underlying substrate is essential for the separation of the oxidation peaks of DA and AA. This might explain why the best response is obtained at electrode modified by the deposition of nickel oxide via two potential cycles. It is likely that the electrodes prepared by one potential cycle do not separate the voltammetric peaks because the underlying gold substrate is exposed to the electrolyte solution by a larger extent, i.e., the response of the gold electrode is controlling the electrochemical process. It is well known that bare gold electrode cannot separate the peaks of DA and AA [20, 21]. In the case of the modified electrode prepared by five potential cycles, the exposed area of the underlying gold substrate becomes very small. Nickel oxide enhances the adsorption of

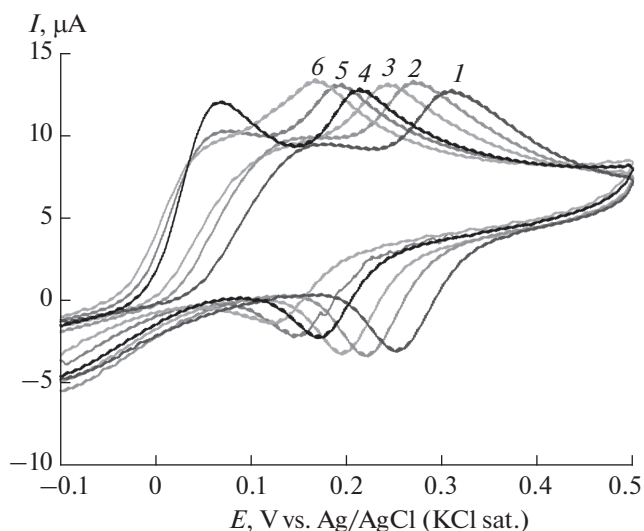
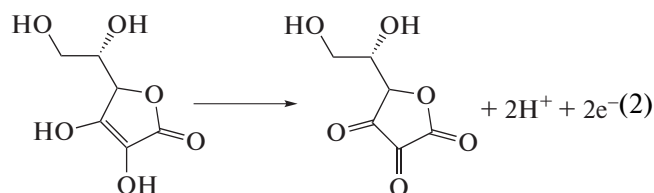
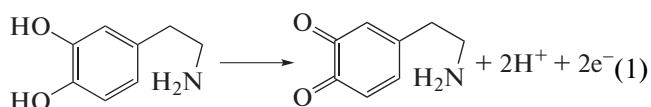


**Fig. 5.** Cyclic voltammograms obtained at nano-NiO<sub>x</sub>/Au electrode in N<sub>2</sub>-saturated phosphate buffer solution containing 0.25 mM DA + 1.0 mM AA. pH: 5.86 (1), 6.04 (2), 6.82 (3), 7.25 (4), 7.62 (5) and 8.03 (6). Scan rate 100 mV/s.

ascorbic acid facilitating its electrochemical oxidation at lower potential. This results in discriminating the electrochemical response of the two species [24]. Similar results have been reported at gold-palladium binary catalyst, acting as a mediator, modified onto glassy carbon electrode for the simultaneous determination of the two species over a wide concentration range extending from mM to μM [25].

Next the effect of pH was optimized. The oxidation of DA (Eq. 1) and AA (Eq. 2) involves protons and thus is expected to be pH dependent. Cyclic voltammograms of DA and AA obtained at nano-NiO<sub>x</sub>/Au electrode in phosphate buffer solutions of different pHs at a scan rate of 100 mV/s are shown in Fig. 5. As clearly shown, the peak potentials of the two species shifted negatively upon increasing the pH. In addition, the peak current slightly increased. The large peak separation is obtained at pH 7.25 (curve 5). At higher pH values the two peaks for the DA and AA oxidation overlap. Thus, pH 7.25 will be used hereafter as the optimum one. Peak potentials extracted from this figure are plotted against pH. A linear plot with a slope equaling 60 mV/pH was obtained (data not shown). The linear dependence of peak potential of DA on pH indicates the presence of a proton-transfer reaction preceding the electrode process. The slope is close to Nernstian, revealing that the uptake of electrons is accompanied by an equal number of protons (Eq. 1). Similar results are obtained for the dependence of the oxidation of AA on pH.



The selectivity of the present determination of DA and AA was examined by measuring the CVs at the nano-NiO<sub>x</sub>/Au electrode for 1.1 mM AA in the presence of different concentrations of DA (data not shown). The oxidation peak current of AA was constant irrespective of the concentration of DA. The negative shift in the well-defined oxidation peak of AA obtained at nano-NiO<sub>x</sub>/Au electrode, in comparison with that at the poly-Au electrode and nano-Ni/Au electrodes, makes possible to selectively determine DA in the presence of AA.

**Square wave voltammetry.** The two peaks of the oxidation of AA and DA are utilized for their selective determination using square wave voltammetry which offers excellent discrimination against double-layer charging current and accordingly has a high sensitivity [26]. First, the instrumental parameters, i.e., step potential, square wave amplitude and frequency, were optimized before recording the square wave voltammograms for the reduction of DA and AA. These parameters are interrelated and have a combined effect on the obtained response. Finally the following parameters were used: step potential, 4 mV, square wave amplitude, 25 mV, and frequency, 25 Hz (and thus the scan rate was 100 mV/s).

Under the optimum conditions and for the sake of comparison, the square wave voltammograms (SWVs) of AA and DA in their coexistence were recorded at nano-NiO<sub>x</sub>/Au electrode in two cases (Fig. 6), i.e. 1<sup>st</sup>, keeping the concentration of AA constant and changing the concentration of DA, and the 2<sup>nd</sup>, the reverse, i.e. keeping the concentration of DA constant while changing the concentration of AA (Fig. 6). As clearly shown in curves 1–4 in which the concentration of AA is kept constant and the concentration of DA is changed, the first peak keeps constant while the peak at 0.2 V (corresponds to DA) is increased. In curves 4–6 the DA concentration is kept constant and that of AA is changed. Again, the peak for AA is increased, while the peak of DA is constant confirming the high selectivity of the present method.

Figure 7 shows SWVs obtained for the oxidation of various concentrations of DA and AA. The oxidation peaks of DA and AA are clearly observed at about 0.2 and 0.02 V, respectively. Based on the SWVs obtained, the linear calibration curves for DA and AA were obtained in N<sub>2</sub>-saturated phosphate buffer solution (pH 7.25) over a wide concentration range and shown as inset. The RSD was less than 1%, indicating good precision of the present method.

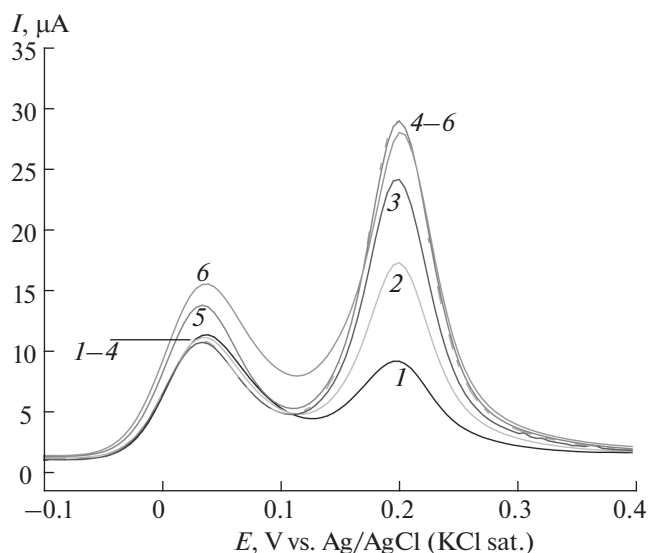


**Fig. 6.** Square wave voltammograms obtained at nano-NiO<sub>x</sub>/Au electrode in N<sub>2</sub>-saturated phosphate buffer solution containing different concentrations of DA and AA mixture: 0.3 mM DA + 1.0 mM AA (1), 0.5 mM DA + 1.0 mM AA (2), 0.6 mM DA + 1.0 mM AA (3), 0.75 mM DA + 1.0 mM AA, 0.75 mM DA + 1.2 mM AA (5) and 0.75 mM DA + 1.4 mM AA (6). Square wave amplitude: 25 mV; frequency: 15 Hz; step potential: 4 mV; quiet time: 2 s. The electrode potential was scanned from -0.1 V to 0.4 V.

The limits of detection (**LOD**) and quantification (**LOQ**) were calculated based on IUPAC's recommendations, from the standard deviation of the response ( $s$ ) and the slope of the calibration curve ( $m$ ) using the following equations [27]:  $\text{LOD} = 3s/m$ ,  $\text{LOQ} = 10s/m$ . The LOD and LOQ for the present electro-determination of DA were calculated as 0.06 and 0.21  $\mu\text{M}$ , respectively, and for AA as 0.23, 0.76  $\mu\text{M}$ , respectively. Analytical parameters for simultaneous determination of DA and AA at the nano-NiO<sub>x</sub>/Au electrode are summarized in Table 1. Relative standard deviations are small, pointing to the high reproducibility of the present method. Statistical data obtained using Student's  $t$ -test shows the high significance of the results obtained by the present method.

Ascorbic acid is the main potential interfering species with dopamine. Results presented above proof the high selectivity of the present method in the determination of DA and AA in their coexistence. The interference expected from other common substances such as glucose, citrate, cysteine, K<sup>+</sup>, Na<sup>+</sup> with dopamine was examined in phosphate buffer of pH 7.25 under the optimum conditions. Tolerance limit was considered as the maximum concentration of the interfering species with a relative error less than 5%. The tolerated

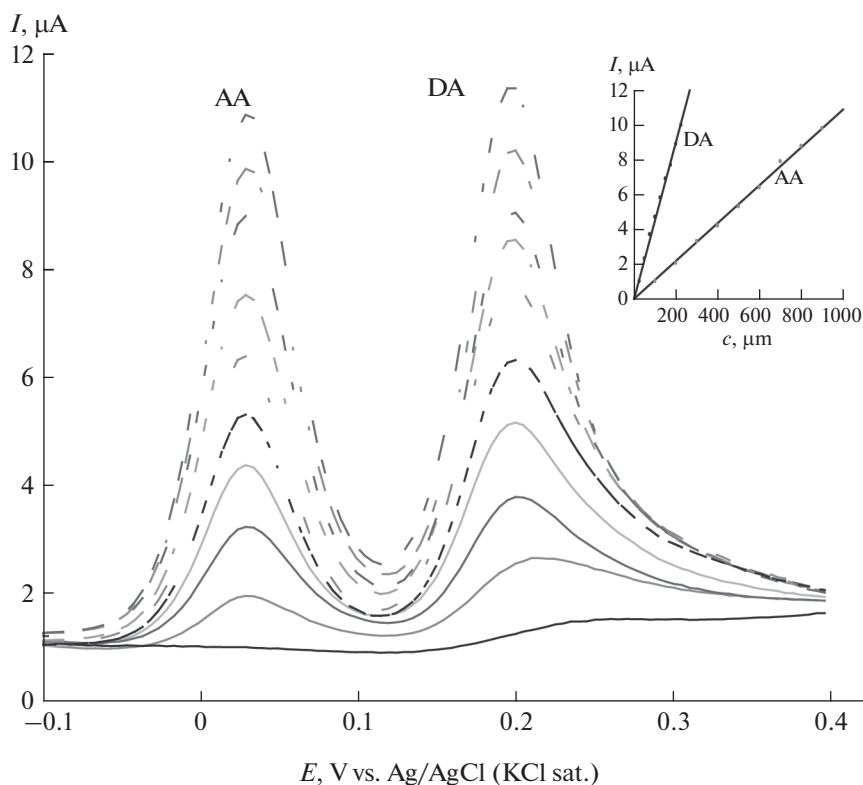


**Fig. 7.** Square wave voltammograms obtained at nano-NiO<sub>x</sub>/Au electrode in N<sub>2</sub>-saturated phosphate buffer solution (pH 7.25) containing different concentrations of AA (0.0, 0.1, 0.2, 0.3, 0.4, 0.5, 0.6, 0.7, 0.8 and 0.9 mM) and DA: [DA] = 0.25[AA]. Square wave amplitude: 25 mV; frequency: 15 Hz; step potential: 4 mV; quiet time: 2 s. The electrode potential was scanned from -0.1 V to 0.4 V. Inset shows calibration curves for DA and AA.

**Table 1.** Analytical parameters of the electroanalytical determination of dopamine and ascorbic acid using square wave voltammetry

Parameter	DA	AA
Optimum buffer	Phosphate	Phosphate
Optimum pH	7.25	7.25
Measured potential, mV	200	30
Scan rate, mV/s	100	100
Linear concentration range, $\mu\text{M}$	20–200	50–900
Slope, $\mu\text{A}/\mu\text{M}$	0.044	0.011
Intercept, $\mu\text{A}$	−0.15	0.166
Correlation coefficient, $R^2$	0.998	0.997
Standard deviation, SD ( $n = 6$ ), $\mu\text{M}$	0.144	0.28
Relative standard deviation, %	0.72	0.94
LOD, $\mu\text{M}$	0.065	0.23
LOQ, $\mu\text{M}$	0.21	0.76
Student's $t$ -test <sup>a</sup>	0.51	0.26

<sup>a</sup> At 95% confidence level, the theoretical  $t$ -value for 5 degrees of freedom is 2.78.

**Table 2.** Simultaneous determination of dopamine and ascorbic acid in model samples

Sample	Added, $\mu\text{M}$		Found <sup>a</sup> , $\mu\text{M}$		Recovery <sup>b</sup> , %	
	DA	AA	DA	AA	DA	AA
1	25	200	25.1	199	100.4 $\pm$ 0.8	99.5 $\pm$ 0.7
2	50	500	50.3	498	100.6 $\pm$ 0.7	99.6 $\pm$ 0.3
3	100	400	100.7	399	101 $\pm$ 1	100 $\pm$ 2

<sup>a</sup> Average of six determinations, <sup>b</sup> mean  $\pm$  SD ( $n = 6$ ).

ratio of the studied interfering species was 500 for  $\text{Na}^+$  and  $\text{K}^+$ ; 30 for glycine, glutamic acid and citrate. Regarding L-cystine, the electrochemical response was obscured due to the formation of self-assembled monolayer via the adsorption of cysteine on the underlying gold substrate [23, 28, 29].

Investigation of the applicability of the proposed method was examined by the determination of the two species in some model samples (Table 2). The recoveries of the spiked standard substances ranged between 99.5 and 100.6%. It becomes clear that the proposed method might be suitable for the simultaneous determination of DA and AA in their coexistence as is characterized by high selectivity and tolerance to possible interfering species.

## CONCLUSIONS

The voltammetric behavior of dopamine and ascorbic acid has been studied at nano-Ni and nano- $\text{NiO}_x$  modified polycrystalline (poly-Au) electrode. Dopamine and ascorbic acid have been selectively and simultaneously determined at nano- $\text{NiO}_x$  modified polycrystalline gold electrode (nano- $\text{NO}_x/\text{Au}$ ) in

phosphate buffer solution (pH 7.25). The loading level of nickel, as well as the oxidation of the deposited nano-Ni have played a prominent role in the simultaneous determination of the two species. The calibration curves for both species have been obtained over an acceptable concentration range with a high correlation coefficient.

## ACKNOWLEDGMENTS

The authors would like to thank Institute of Scientific Research and Revival of Islamic Heritage at Umm Al-Qura University (Project ID 43405076) for the financial support.

## REFERENCES

1. Thomas, T., Mascarenhas, R.J., Kumara Swamy, B.E., Martis, P., Mekhalif, Z., and Sherigara B.S., *Colloids Surf., B*, 2013, vol. 110, p. 458.
2. André, C., Castanheira, I., Cruz, J.M., Paseiro, P., and Sanches-Silva, A., *Trends Food Sci. Technol.*, 2010, vol. 21, p. 229.

3. Noroozifar, M., Khorasani-Motlagh, M., Akbaria, R., and Parizi, M.B., *Biosens. Bioelectron.*, 2011, vol. 28, p. 56.
4. Etesami, M. and Mohamed, N., *Int. J. Electrochem. Sci.*, 2011, vol. 6, p. 4676.
5. Danial, A.S., Saleh, M.M., Salih, S.A., and Awad, M.I., *J. Power Sources*, 2015, vol. 293, p. 101.
6. Kassem, M.A., Hazazi, O.A., Ohsaka, T., and Awad, M.I., *Electroanalysis*, 2016, vol. 28, p. 539.
7. El-Refaei, S.M., Saleh, M.M., and Awad, M.I., *J. Solid State Electrochem.*, 2014, vol. 18, p. 5.
8. El-Refaei, S.M., Saleh, M.M., and Awad, M.I., *J. Power Sources*, 2013, vol. 223, p. 125.
9. Awad, M.I., El-Deab, M.S., and Ohsaka, T., *J. Electrochem. Soc.*, 2007, vol. 154, no. 8, p. B810.
10. Capella, P., Ghasemzadeh, B., Mitchell, K., and Adams, R.N., *Electroanalysis*, 1990, vol. 2, p. 175.
11. Justice, J.B., Jr. and Jaramillo, A., *J. Electrochem. Soc.*, 1984, vol. 131, p. 106C.
12. Zhu, R.H. and Kok, W.T., *Anal. Chem.*, 1997, vol. 69, p. 4010.
13. Chernyshov, D.V., Shuedene, N.V., Antipova, E.R., and Pletnev, I.V., *Anal. Chim. Acta*, 2008, vol. 621, p. 178.
14. Li, L.L., Liu, H.Y., Shen, Y.Y., Zhang, J.R., and Zhu, J.J., *Anal. Chem.*, 2011, vol. 83, p. 661.
15. Yoshitake, T., Kehr, J., Todoroki, K., Nohta, H., and Yamaguchi, M., *Biomed. Chromatogr.*, 2006, vol. 20, p. 267.
16. Lei, Z., Jia, J.B., Zou, X.Q., and Dong, S.J., *Electroanalysis*, 2004, vol. 16, p. 1413.
17. Park, J.Y., Myung, S.W., Kim, I.S., Choi, D.-K., Kwon, S.J., and Yoon, S.H., *Biol. Pharm. Bull.*, 2013, vol. 36, p. 252.
18. Han, H.S., Lee, H.K., You, J.M., Jeong, H., and Jeon, S., *Sens. Actuators, B*, 2014, vol. 190, p. 886.
19. Rand, E., Periyakaruppan, A., Tanaka, Z., Zhang, D.A., Marsh, M.P., Andrews, R.J., Lee, K.H., Chen, B., Meyyappan, M., and Koehne, J.E., *Biosens. Bioelectron.*, 2013, vol. 42, p. 434.
20. Raj, C.R. and Ohsaka, T., *Electrochem. Commun.*, 2001, vol. 11, p. 633.
21. Raj, C.R. and Ohsaka, T., *Bioelectrochemistry*, 2001, vol. 53, p. 251.
22. Moharana, M. and Mallik, A., *Electrochim. Acta*, 2013, vol. 98, p. 1.
23. Awad, M.I. and Ohsaka, T., *Sens. Actuators, B*, 2015, vol. 221, p. 1335.
24. Hutton, L.A., Vidotti, M., Patel, A.N., Newton, M.E., Unwin, P.R., and Macpherson, J.V., *J. Phys. Chem. C*, 2011, vol. 115, p. 1649.
25. Shaidarova, L.G., Chelnokova, I.A., Gedmina, A.V., and Budnikov, G.K., *J. Anal. Chem.*, 2009, vol. 64, p. 36.
26. Babaei, A., Aminikhah, M., and Taheri, A.R., *Sens. Lett.*, 2013, vol. 11, p. 413.
27. Murray, R.W., in *Electroanalytical Chemistry*, vol. 13, Bard, A.J., Ed., New York: Marcel Dekker, 1984, p. 191.
28. Awad, M.I. and Ohsaka, T., *J. Power Sources*, 2013, vol. 226, p. 306.
29. Awad, M.I., *Anal. Chim. Acta*, 2012, vol. 730, p. 60

SPELL: 1. OK